Finite Horizon Robustness Analysis of LTV Systems Using Integral Quadratic Constraints

Peter Seiler [a], Robert M. Moore [b], Chris Meissen [b], Murat Arcak [c], and Andrew Packard [b]

[a] *Department of Aerospace Engineering and Mechanics at the University of Minnesota*

[b] *Department of Mechanical Engineering at the University of California, Berkeley*

[c] *Department of Electrical Engineering and Computer Science at the University of California, Berkeley*

Abstract

The goal of this paper is to assess the robustness of an uncertain linear time-varying (LTV) system on a finite time horizon. The uncertain system is modeled as an interconnection of a known LTV system and a perturbation. The input/output behavior of the perturbation is described by time-domain, integral quadratic constraints (IQCs). Typical notions of robustness, e.g. nominal stability and gain/phase margins, can be insufficient for finite-horizon analysis. Instead, this paper focuses on robust induced gains and bounds on the reachable set of states. Sufficient conditions to compute robust performance bounds are formulated using dissipation inequalities and IQCs. The analysis conditions are provided in two equivalent forms as Riccati differential equations and differential linear matrix inequalities, and an algorithm is developed leveraging both forms.

Key words: Robustness; Integral Quadratic Constraints; Linear Time Varying

1 Introduction

This paper develops theoretical and computational methods to analyze the robustness of linear time-varying (LTV) systems over finite time horizons. Motivating applications which undergo finite-time trajectories include robotic systems (Murray et al., 1994) and space launch vehicles (Marcos and Bennani, 2009). Typical notions of robustness, e.g. nominal stability and gain/phase margins, can be insufficient for such systems. For example, evaluating the stability of the LTV system at "frozen" time instances can lead to erroneous conclusions, since there are unstable LTV systems $\dot{x}(t) = A(t)x(t)$ for which $A(t)$ is stable at each frozen time t (Khalil, 2001).

The analysis in this paper is performed on an uncertain LTV system modeled by an interconnection of a known, nominal LTV system G and a perturbation Δ, as in Figure 1. The perturbation may model nonlinearities and dynamic or parametric uncertainty. The input-output properties of Δ are characterized by integral quadratic constraints (IQCs) (Megretski and Rantzer, 1997). An extensive list of IQCs for various classes of perturbations is given in (Megretski and Rantzer, 1997; Veenman et al., 2016). The main result in Megretski and Rantzer (1997) is an infinite-horizon, input-output $\mathcal{L}_2$ stability theorem using frequency domain IQCs.

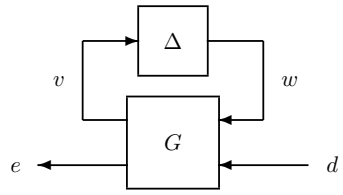

Fig. 1. Interconnection $F_u(G, \Delta)$ of a nominal LTV system G and perturbation Δ.

The main contribution of this paper is an algorithm to compute finite horizon robustness metrics including the effects of exogenous disturbances. First, nominal finite-horizon LTV performance is reviewed (Section 2) focus-

⋆ The authors acknowledge funding from ONR project N00014-18-1-2209. This paper was not presented at any IFAC meeting. Corresponding author P. Seiler.

Email addresses: seile017@umn.edu (Peter Seiler), max.moore@raytheon.com (Robert M. Moore), cmeissen@berkeley.edu (Chris Meissen), arcak@berkeley.edu (Murat Arcak), apackard@berkeley.edu (Andrew Packard).

ing on induced $\mathcal{L}_2$ and $\mathcal{L}_2$-to-Euclidean gains. Next, conditions are given (Section 3) to bound these performance metrics for uncertain LTV systems. The analysis uses dissipation inequalities and IQCs leading to differential linear matrix inequality (DLMI) conditions. The DLMI is equivalent to a Riccati Differential Equation (RDE) by a variation of the strict bounded real lemma (Theorem 1 in Section 2), which generalizes results in (Tadmor, 1990; Ravi et al., 1991; Green and Limebeer, 1995; Chen and Tu, 2000; Başar and Bernhard, 2008). Finally, algorithm 1 in Section 4.4 is proposed to compute bounds on the finite horizon robustness metrics. The approach is demonstrated with two examples (Section 5).

A second contribution is that the proposed algorithm combines the complementary benefits of the DLMI and RDE conditions. Both conditions involve a storage function matrix $P(t)$ and variables to parameterize the IQC. The benefit of the DLMI is that it is convex in P and the IQC variables. The drawback is that it is an infinite dimensional constraint due to the dependence on t and $P(t)$. This was "approximately" solved in (Moore, 2015) as a finite-dimensional convex optimization by enforcing the DLMI on a time grid and parameterizing $P(t)$ using basis functions. However there are no formal guarantees, in general, with these approximations. [1] In contrast, the RDE directly solves for $P(t)$ given values of the IQC variables. This avoids approximations due to time gridding and basis functions for $P(t)$. The RDE also yields a rigorous performance bound if a solution exists on $[0,T]$. The drawback is that the RDE has a rational (non-convex) dependence on the IQC variables.

Finite-horizon robustness of LTV systems using IQCs is also considered in (Jönsson, 2002; Petersen et al., 2000). There are two main distinctions with the results in this paper. First, these prior works account for initial conditions but neglect exogenous disturbances. Second, they both propose optimizing directly over the IQC variables focusing on the RDE condition. This is inefficient if the IQC is parameterized by many variables, e.g. see Remark 6.2.4 in Petersen et al. (2000). As noted above, our proposed algorithm exploits the complementary benefits of the RDE and DLMI conditions.

Notation: $\mathbb{R}^{n\times m}$ and $\mathbb{S}^n$ denote the sets of n-by-m real matrices and n-by-n real, symmetric matrices. The finite-horizon $\mathcal{L}_2[0,T]$ norm of a signal $v:[0,T]\to\mathbb{R}^n$ is $\|v\|_{2,[0,T]} := \left(\int_0^T v(t)^T v(t)dt\right)^{1/2}$. If $\|v\|_{2,[0,T]} < \infty$ then $v \in \mathcal{L}_2[0,T]$. $\mathbb{RL}_\infty$ is the set of rational functions with real coefficients that have no poles on the imaginary axis. $\mathbb{RH}_\infty \subset \mathbb{RL}_\infty$ contains functions that are analytic in the closed right-half of the complex plane.

[1] Similar approximations are used for analysis of "gridded" linear parameter varying (LPV) systems. See closely related work on uncertain LPV systems in Pfifer and Seiler (2016). These approximations yield rigorous bounds in special cases. For example, Masubuchi et al. (1998) consider nominal LPV systems with piecewise linear dependence on the parameters. The main result is a rigorous bound on the induced $\mathcal{L}_2$ gain using smoothed first-order spline bases functions for P and a sufficiently dense gridding of the parameter space.

2 Nominal Performance

2.1 Finite Horizon LTV Systems

Consider an LTV system G defined on $[0,T]$:

$$\dot{x}(t) = A(t)x(t) + B(t)d(t) \tag{1}$$
$$e(t) = C(t)x(t) + D(t)d(t) \tag{2}$$

$x \in \mathbb{R}^{n_x}$ is the state, $d \in \mathbb{R}^{n_d}$ is the input, and $e \in \mathbb{R}^{n_e}$ is the output. The state matrices $A:[0,T]\to\mathbb{R}^{n_x\times n_x}$, $B:[0,T]\to\mathbb{R}^{n_x\times n_d}$, $C:[0,T]\to\mathbb{R}^{n_e\times n_x}$, and $D:[0,T]\to\mathbb{R}^{n_e\times n_d}$ are piecewise-continuous (bounded) functions of time. It is assumed throughout that $T<\infty$. Thus $d\in\mathcal{L}_2[0,T]$ implies x and e are in $\mathcal{L}_2[0,T]$ for any $x(0)$ (Brockett, 2015).

Many different performance metrics can be defined for this (nominal) finite-horizon LTV system. This paper mainly focuses on two specific metrics. First, the *finite-horizon induced $\mathcal{L}_2$-gain* of G is

$$\|G\|_{2,[0,T]} := \sup\left\{ \frac{\|e\|_{2,[0,T]}}{\|d\|_{2,[0,T]}} \;\middle|\; x(0)=0, 0\neq d\in\mathcal{L}_{2,[0,T]} \right\}.$$

As noted above, $d\in\mathcal{L}_2[0,T]$ implies $e\in\mathcal{L}_2[0,T]$. Thus the $\mathcal{L}_2$ gain is finite for any fixed horizon $T<\infty$. Next, assume $D(T)=0$. Then the *finite-horizon $\mathcal{L}_2$-to-Euclidean gain* of G is

$$\|G\|_{E,[0,T]} := \sup\left\{ \frac{\|e(T)\|_2}{\|d\|_{2,[0,T]}} \;\middle|\; x(0)=0, 0\neq d\in\mathcal{L}_{2,[0,T]} \right\}.$$

The $\mathcal{L}_2$-to-Euclidean gain depends on the system output e only at the final time T. The assumption that $D(T)=0$ ensures this gain is well-defined. The $\mathcal{L}_2$-to-Euclidean gain can be used to bound the set of states $x(T)$ reachable by disturbances of a given norm. This *reachable set* is formally defined as follows:

$$\mathcal{R}_\beta := \left\{ x(T) \;\middle|\; x(0)=0, \|d\|_{2,[0,T]}\le\beta \right\}. \tag{3}$$

If $C(T)=I_{n_x}$ and $D(T)=0$ then $e(T)=x(T)$. In this case, if $\|G\|_{E,[0,T]}\le\gamma$ then $\|x(T)\|_2\le\gamma\|d\|_{2,[0,T]}$ and hence $\mathcal{R}_\beta$ is contained in a sphere of radius $\gamma\beta$. More general ellipsoidal bounds on $\mathcal{R}_\beta$ can also be computed. Select $C := E^{\frac{1}{2}}$ and $D:=0$ for some given $E\in\mathbb{S}^{n_x}$ with $E\succeq 0$. With these choices $\|G\|_{E,[0,T]}\le\gamma$ implies the ellipsoidal bound $\mathcal{R}_\beta \subseteq \{x\in\mathbb{R}^n \mid x^TEx\le\beta^2\gamma^2\}$. Note that the reachable set $\mathcal{R}_\beta$, as defined in Equation 3, bounds the state only at the final time T. The state $x(t)$ at intermediate times $t\in[0,T]$ can similarly be bounded using the $\mathcal{L}_2$-to-Euclidean gain $\|G\|_{E,[0,t]}$.

2.2 Generic Quadratic Cost

The two nominal performance metrics introduced above are generalized in Section 3 to assess robustness of uncertain systems. A generic quadratic cost function is defined next to unify these various cases. Let $Q : [0,T] \to \mathbb{S}^{n_x}$, $R : [0,T] \to \mathbb{S}^{n_d}$, $S : [0,T] \to \mathbb{R}^{n_x \times n_d}$, and $F \in \mathbb{R}^{n_x \times n_x}$ be given. (Q,S,R) are assumed to be piecewise continuous (bounded) functions. A quadratic cost function $J : \mathcal{L}_2[0,T] \to \mathbb{R}$ is defined by (Q,S,R,F) as follows:

$$J(d) := x(T)^T F x(T) + \int_0^T \begin{bmatrix} x(t) \\ d(t) \end{bmatrix}^T \begin{bmatrix} Q(t) & S(t) \\ S(t)^T & R(t) \end{bmatrix} \begin{bmatrix} x(t) \\ d(t) \end{bmatrix} dt$$
$$\text{subject to: Eq. 1 with } x(0) = 0 \qquad (4)$$

The finite-horizon induced $\mathcal{L}_2$ gain of G can be related to the quadratic cost J by proper choice of (Q,S,R,F). Let $\gamma > 0$ be given and select $Q(t) := C(t)^T C(t)$, $S(t) := C(t)^T D(t)$, $R(t) := D(t)^T D(t) - \gamma^2 I_{n_d}$, and $F := 0$. This yields the cost function $J(d) := \|e\|^2_{2,[0,T]} - \gamma^2 \|d\|^2_{2,[0,T]}$. Thus $J(d) \le 0 \, \forall d \in \mathcal{L}_2[0,T]$ if and only if $\|G\|_{2,[0,T]} \le \gamma$. The finite-horizon $\mathcal{L}_2$-to-Euclidean gain of G can also be related to J: let $\gamma > 0$ be given and select $Q(t) := 0$, $S(t) := 0$, $R(t) := -\gamma^2 I_{n_d}$, and $F := C^T(T)C(T)$. This yields $J(d) := \|e(T)\|_2^2 - \gamma^2 \|d\|^2_{2,[0,T]}$, and $J(d) \le 0 \, \forall d \in \mathcal{L}_2[0,T]$ if and only if $\|G\|_{E,[0,T]} \le \gamma$.

2.3 Strict Bounded Real Lemma

The next theorem states an equivalence between a bound on the quadratic cost J and the existence of a solution to a Riccati Differential Equation (RDE) or Riccati Differential Inequality (RDI). The theorem generalizes existing results for the induced $\mathcal{L}_2$ gain of LTV systems (Tadmor, 1990; Ravi et al., 1991; Green and Limebeer, 1995; Chen and Tu, 2000; Başar and Bernhard, 2008). The corresponding conditions for LTI systems and infinite-horizon performance are specified in terms of algebraic Riccati equations and inequalities (Zhou et al., 1996).

Theorem 1 *Let (Q,S,R,F) be given with $R(t) \prec 0$ for all $t \in [0,T]$. The following statements are equivalent:*

(1) $\exists \epsilon > 0$ such that $J(d) \le -\epsilon \|d\|^2_{2,[0,T]} \; \forall d \in \mathcal{L}_2[0,T]$.

(2) There exists a differentiable function $Y : [0,T] \to \mathbb{S}^n$ such that $Y(T) = F$ and

$$\dot{Y} + A^T Y + Y A + Q - (YB + S) R^{-1} (YB + S)^T = 0$$

This is a Riccati Differential Equation (RDE).

(3) There exists $\epsilon > 0$ and a differentiable function $P : [0,T] \to \mathbb{S}^n$ such that $P(T) \succeq F$ and

$$\dot{P} + A^T P + PA + Q - (PB + S) R^{-1} (PB + S)^T \preceq -\epsilon I$$

This is a strict Riccati Differential Inequality (RDI).

PROOF. **(3 ⇒ 1)** By Schur complements (Boyd et al., 1994), the RDI and $R(t) \prec 0$ imply $\exists \tilde{\epsilon} > 0$ such that

$$\begin{bmatrix} \dot{P} + A^T P + PA & PB \\ B^T P & 0 \end{bmatrix} + \begin{bmatrix} Q & S \\ S^T & R \end{bmatrix} \preceq -\tilde{\epsilon} I \qquad (5)$$

Let $x(t)$ be a solution of the LTV system (Equation 1) starting from $x(0) = 0$ and forced by $d \in \mathcal{L}_2[0,T]$. Multiply Equation 5 on the left and right by $[x(t)^T \; d(t)^T]$ and its transpose. This yields the following dissipation inequality with storage function $V(x,t) := x^T P(t) x$:

$$\dot{V} + \begin{bmatrix} x \\ d \end{bmatrix}^T \begin{bmatrix} Q & S \\ S^T & R \end{bmatrix} \begin{bmatrix} x \\ d \end{bmatrix} \le -\tilde{\epsilon} \begin{bmatrix} x \\ d \end{bmatrix}^T \begin{bmatrix} x \\ d \end{bmatrix} \qquad (6)$$

Integrate the dissipation inequality from $t = 0$ to $t = T$:

$$V(x(T),T) - V(x(0),0) + \int_0^T \begin{bmatrix} x(t) \\ d(t) \end{bmatrix}^T \begin{bmatrix} Q(t) & S(t) \\ S(t)^T & R(t) \end{bmatrix} \begin{bmatrix} x(t) \\ d(t) \end{bmatrix} dt \le -\tilde{\epsilon} \left\| \begin{bmatrix} x \\ d \end{bmatrix} \right\|^2_{2,[0,T]}$$

Apply the boundary condition $P(T) \succeq F$ to obtain:

$$J(d) \le V(x(0),0) - \tilde{\epsilon} \|d\|^2_{2,[0,T]} \qquad (7)$$

This bound is valid for any $d \in \mathcal{L}_2[0,T]$. Hence, applying $x(0) = 0$ yields $J(d) \le -\tilde{\epsilon} \|d\|^2_{2,[0,T]} \; \forall d \in \mathcal{L}_2[0,T]$.

The proof of $(1 \Rightarrow 2)$, $(2 \Rightarrow 1)$, $(1 \Rightarrow 3)$ is given in (Seiler et al., 2017). It is similar to that given in Section 3.7.4 of (Green and Limebeer, 1995) for the special case of finite-horizon induced $\mathcal{L}_2$ gains. □

Nominal performance is most easily assessed using the RDE. The performance $J(d) \le -\epsilon \|d\|^2_{2,[0,T]}$ is achieved if the associated RDE exists on $[0,T]$ when integrated backward from $Y(T) = F$. The assumption $R(t) \prec 0$ ensures $R(t)$ is invertible and hence the RDE is well-defined $\forall t \in [0,T]$. Thus the solution of the RDE exists on $[0,T]$ unless it grows unbounded. As an example, $J(d) := \|e\|^2_{2,[0,T]} - \gamma^2 \|d\|^2_{2,[0,T]}$ for specific choices of (Q,S,R,F) where R depends on the choice of γ. For a fixed $\gamma > 0$, the performance $\|G\|_{2,[0,T]} < \gamma$ is achieved if the associated RDE exists on $[0,T]$ when integrated backward from $Y(T) = 0$. The smallest bound on the induced $\mathcal{L}_2$ gain is found via bisection. The RDI is used later to assess the robustness of uncertain LTV systems.

3 Robust Performance

3.1 Uncertain LTV Systems

An uncertain, finite-horizon LTV system is given by the interconnection $F_u(G,\Delta)$ of a nominal LTV system G

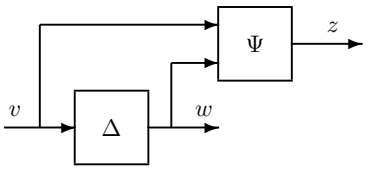

Fig. 2. Graphical interpretation for time domain IQCs

and a perturbation Δ as shown in Figure 1. The LTV system G is described by the following state-space model:

$$\begin{aligned} \dot{x}_G(t) &= A_G(t)\,x_G(t) + B_{G1}(t)\,w(t) + B_{G2}(t)\,d(t) \\ v(t) &= C_{G1}(t)\,x_G(t) + D_{G11}(t)\,w(t) + D_{G12}(t)\,d(t) \\ e(t) &= C_{G2}(t)\,x_G(t) + D_{G21}(t)\,w(t) + D_{G22}(t)\,d(t) \end{aligned} \quad (8)$$

where $x_G \in \mathbb{R}^{n_G}$ is the state. The inputs are $w \in \mathbb{R}^{n_w}$ and $d \in \mathbb{R}^{n_d}$ while $v \in \mathbb{R}^{n_v}$ and $e \in \mathbb{R}^{n_e}$ are outputs. The state matrices are piecewise continuous (bounded) functions of time with appropriate dimensions, e.g. $A_G : [0,T] \to \mathbb{R}^{n_G \times n_G}$. The perturbation is an operator $\Delta : \mathcal{L}_2^{n_v}[0,T] \to \mathcal{L}_2^{n_w}[0,T]$. Well-posedness of the interconnection $F_u(G,\Delta)$ is defined as follows.

Definition 2 *$F_u(G,\Delta)$ is well-posed if for all $x_G(0) \in \mathbb{R}^{n_G}$ and $d \in \mathcal{L}_2^{n_d}[0,T]$ there exists unique solutions $x_G \in \mathcal{L}_2^{n_G}[0,T]$, $v \in \mathcal{L}_2^{n_v}[0,T]$, $e \in \mathcal{L}_2^{n_e}[0,T]$, and $w \in \mathcal{L}_2^{n_w}[0,T]$ satisfying Equation (8) and $w = \Delta(v)$ with a causal dependence on d.*

The perturbation Δ can have block-structure as is standard in robust control modeling (Zhou et al., 1996). It can include blocks that are hard nonlinearities (e.g. saturations) and infinite dimensional operators (e.g. time delays) in addition to true system uncertainties. The term "uncertainty" is used for simplicity when referring to Δ.

3.2 Integral Quadratic Constraints (IQCs)

IQCs (Megretski and Rantzer, 1997) are used to describe the input/output behavior of Δ. They can be formulated in either the frequency or time domain. The time domain formulation (Petersen et al., 2000) is more useful for analysis of uncertain time-varying systems. This formulation is based on the graphical interpretation in Figure 2. The inputs and outputs of Δ are filtered through an LTI system Ψ with zero initial condition $x_\psi(0) = 0$. The dynamics of Ψ are given as follows:

$$\begin{aligned} \dot{x}_\psi(t) &= A_\psi\,x_\psi(t) + B_{\psi 1}\,v(t) + B_{\psi 2}\,w(t) \\ z(t) &= C_\psi\,x_\psi(t) + D_{\psi 1}\,v(t) + D_{\psi 2}\,w(t) \end{aligned} \quad (9)$$

where $x_\psi \in \mathbb{R}^{n_\psi}$ is the state. A time domain IQC is an inequality enforced on the output z over a finite horizon. The formal definition is given next.

Definition 3 *Let $\Psi \in \mathbb{RH}_\infty^{n_z \times (n_v+n_w)}$ and $M : [0,T] \to \mathbb{S}^{n_z}$ be given with M piecewise continuous. An operator $\Delta : \mathcal{L}_2^{n_v}[0,T] \to \mathcal{L}_2^{n_w}[0,T]$ satisfies the time domain IQC defined by (Ψ, M) if the following inequality holds for all $v \in \mathcal{L}_2^{n_v}[0,T]$ and $w = \Delta(v)$:*

$$\int_0^T z(t)^T M(t) z(t)\,dt \;\geq 0 \quad (10)$$

where z is the output of Ψ driven by inputs (v,w) with zero initial conditions $x_\psi(0) = 0$.

The notation $\Delta \in \mathcal{I}(\Psi, M)$ is used when Δ satisfies the corresponding IQC. Time domain IQCs, as defined above, are specified as finite-horizon constraints on the outputs of Ψ. These are often referred to as hard IQCs. The definition given here only requires the IQC to hold over the analysis horizon $[0,T]$. This is in contrast to hard IQCs used for infinite horizon analysis which require the constraint to hold over all finite time horizons. Two examples of time domain IQCs are provided below.

Example 4 *Consider an LTI uncertainty $\Delta \in \mathbb{RH}_\infty$ with $\|\Delta\|_\infty \leq 1$. Let $\Pi_{11} \in \mathbb{RL}_\infty$ be given with $\Pi_{11}(j\omega) = \Pi_{11}(j\omega)^* \geq 0$ for all $\omega \in \mathbb{R} \cup \{+\infty\}$. Then the following frequency domain IQC holds $\forall v \in \mathcal{L}_2^{n_v}$ and $w = \Delta(v)$*

$$\int_{-\infty}^{\infty} \begin{bmatrix} V(j\omega) \\ W(j\omega) \end{bmatrix}^* \underbrace{\begin{bmatrix} \Pi_{11}(j\omega) & 0 \\ 0 & -\Pi_{11}(j\omega) \end{bmatrix}}_{:=\Pi(j\omega)} \begin{bmatrix} V(j\omega) \\ W(j\omega) \end{bmatrix} d\omega \geq 0$$

where V and W are Fourier transforms of v and w. This IQC corresponds to D-scales used in structured singular value μ analysis (Packard and Doyle, 1993; Zhou et al., 1996). A factorized representation for Π yields a valid time domain IQC. Specifically, let $\Pi = \Psi^\sim M \Psi$ where

$$\begin{aligned} \Psi &:= \begin{bmatrix} \Psi_{11} & 0 \\ 0 & \Psi_{11} \end{bmatrix} \text{ with } \Psi \in \mathbb{RH}_\infty^{n_z \times 1} \\ M &:= \begin{bmatrix} M_{11} & 0 \\ 0 & -M_{11} \end{bmatrix} \text{ with } M \in \mathbb{S}^{n_z} \text{ and } M_{11} \succeq 0 \end{aligned} \quad (11)$$

It is shown in (Balakrishnan, 2002) that (Ψ, M) is a valid time domain IQC for Δ over any finite horizon $T < \infty$.

Example 5 *Time domain IQCs are often specified with Ψ as an LTI system and M as a constant matrix. Definition 3 above allows M to be time-varying. This generalization is useful for time-varying real parameters. Let $\Delta := \delta(t)$ where $\delta(t) \in \mathbb{R}$ and $|\delta(t)| \leq 1$ for all $t \in [0,T]$. Define $\Psi := I_2$ and $M(t) := \begin{bmatrix} m_{11}(t) & 0 \\ 0 & -m_{11}(t) \end{bmatrix}$ where $m_{11} : [0,T] \to \mathbb{R}$ is piecewise continuous and satisfies $m_{11}(t) \geq 0$. Then Δ satisfies the time domain IQC defined by (Ψ, M). Time-varying IQCs can be defined for other uncertainties (Pfifer and Seiler, 2015).*

A library of IQCs is provided in Megretski and Rantzer (1997) for various types of perturbations. Most IQCs are for bounded, causal operators with multipliers Π specified in the frequency domain. Under mild assumptions, a

valid time-domain IQC (Ψ, M) can be constructed from Π via a J-spectral factorization (Seiler, 2015). This allows the library of known (frequency domain) IQCs to be used for time-domain, finite-horizon analysis. More general IQC parameterizations are not necessarily "hard" but can be handled as in Fetzer et al. (2017).

3.3 Robust Induced $\mathcal{L}_2$ Gain

The robustness of $F_u(G,\Delta)$ is analyzed using the system shown in Figure 3. This interconnection includes the IQC filter Ψ but the uncertainty Δ has been removed. The precise relation $w = \Delta(v)$ is replaced, for the analysis, by the constraint on the filter output z. The extended system of G (Equation 8) and Ψ (Equation 9) is governed by the following state space model:

$$\begin{aligned} \dot{x}(t) &= \mathcal{A}(t)\,x(t) + \mathcal{B}(t)\begin{bmatrix} w(t) \\ d(t)\end{bmatrix} \\ z(t) &= \mathcal{C}_1(t)\,x(t) + \mathcal{D}_1(t)\begin{bmatrix} w(t) \\ d(t)\end{bmatrix} \\ e(t) &= \mathcal{C}_2(t)\,x(t) + \mathcal{D}_2(t)\begin{bmatrix} w(t) \\ d(t)\end{bmatrix}. \end{aligned} \tag{12}$$

The extended state vector is $x := \left[\begin{smallmatrix} x_G \\ x_\psi\end{smallmatrix}\right] \in \mathbb{R}^n$ where $n := n_G + n_\psi$. The state-space matrices are given by (dropping the dependence on time t):

$$\mathcal{A} := \begin{bmatrix} A_G & 0 \\ B_{\psi 1}C_{G1} & A_\psi \end{bmatrix},\ \mathcal{B} := \begin{bmatrix} B_{G1} & B_{G2} \\ B_{\psi 1}D_{G11} + B_{\psi 2} & B_{\psi 1}D_{G12}\end{bmatrix}$$
$$\mathcal{C}_1 := \begin{bmatrix} D_{\psi 1}C_{G1} & C_\psi \end{bmatrix},\ \mathcal{C}_2 := \begin{bmatrix} C_{G2} & 0\end{bmatrix},$$
$$\mathcal{D}_1 := \begin{bmatrix} D_{\psi 1}D_{G11} + D_{\psi 2} & D_{\psi 1}D_{G12}\end{bmatrix}$$
$$\mathcal{D}_2 := \begin{bmatrix} D_{G21} & D_{G22}\end{bmatrix}.$$

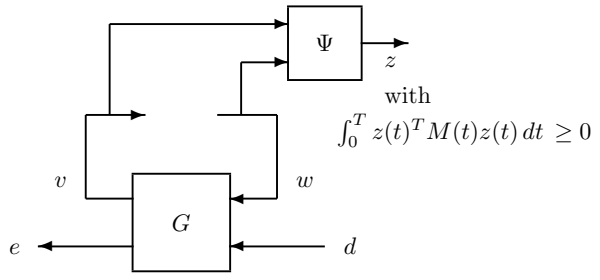

Fig. 3. Extended LTV system of G and filter Ψ.

The actual system to be analyzed is $F_u(G,\Delta)$ with input d and initial condition $x_G(0) = x_{G,0}$. The analysis is instead performed with the extended LTV system (Equation 12) and the constraint $\Delta \in \mathcal{I}(\Psi, M)$. The constrained extended system has inputs (d, w) and initial condition $x(0) = \left[\begin{smallmatrix} x_{G,0} \\ 0\end{smallmatrix}\right]$. The IQC implicitly constrains the input w. *The IQC covers Δ such that the constrained extended system without Δ includes all behaviors of the original system $F_u(G,\Delta)$.*

The following differential matrix inequality is used to assess the robust performance of $F_u(G,\Delta)$ [2]:

$$\begin{bmatrix} \dot{P} + \mathcal{A}^T P + P\mathcal{A} & P\mathcal{B} \\ \mathcal{B}^T P & 0 \end{bmatrix} + \begin{bmatrix} Q & S \\ S^T & R\end{bmatrix} + (\cdot)^T M \begin{bmatrix} \mathcal{C}_1 & \mathcal{D}_1 \end{bmatrix} \preceq -\epsilon I. \tag{13}$$

This inequality depends on the extended system, IQC, and quadratic cost (Q, S, R, F). It is compactly denoted as $DLMI_{Rob}(P, M, \gamma^2, t) \preceq -\epsilon I$. This notation emphasizes that the constraint is a differential linear matrix inequality (DLMI) in (P, M, γ^2) for fixed (G, Ψ) and (Q, S, R, F). The dependence on (G, Ψ) and (Q, S, R, F) is not explicitly denoted but will be clear from context.

The next theorem formulates a sufficient condition to bound the (robust) induced $\mathcal{L}_2$ gain of $F_u(G,\Delta)$. The proof uses IQCs and a standard dissipation argument (van der Schaft, 1999; Willems, 1972a,b; Khalil, 2001). For induced $\mathcal{L}_2$ gains the quadratic cost matrices are chosen as $F := 0$ and

$$\begin{aligned} &Q(t) := \mathcal{C}_2(t)^T\mathcal{C}_2(t),\ \ S(t) := \mathcal{C}_2(t)^T\mathcal{D}_2(t) \\ &R(t) := \mathcal{D}_2(t)^T\mathcal{D}_2(t) - \gamma^2 \begin{bmatrix} 0_{n_w} & 0 \\ 0 & I_{n_d}\end{bmatrix} \end{aligned} \tag{14}$$

Theorem 6 *Let G be an LTV system defined by (8) and $\Delta : \mathcal{L}_2^{n_v}[0,T] \to \mathcal{L}_2^{n_w}[0,T]$ be an operator. Assume $F_u(G,\Delta)$ is well-posed and $\Delta \in \mathcal{I}(\Psi, M)$. If there exists $\epsilon > 0, \gamma > 0$ and a differentiable function $P : [0,T] \to \mathbb{S}^n$ such that $P(T) \succeq F$ and*

$$DLMI_{Rob}(P, M, \gamma^2, t) \preceq -\epsilon I \quad \forall t \in [0,T], \tag{15}$$

then $\|F_u(G,\Delta)\|_{2,[0,T]} < \gamma$.

PROOF. Let $d \in \mathcal{L}_2[0,T]$ and $x_G(0) = x_{G,0}$ be given. By well-posedness, $F_u(G,\Delta)$ has a unique solution (x_G, v, w, e). Define $x := \left[\begin{smallmatrix} x_G \\ x_\psi\end{smallmatrix}\right]$. Then (x, z, e) are a solution of the extended system (12) with inputs (w, d) and initial condition $x(0) = \left[\begin{smallmatrix} x_{G,0} \\ 0\end{smallmatrix}\right]$. Moreover, z satisfies the the IQC defined by (Ψ, M).

Define a storage function by $V(x,t) := x^T P(t) x$. Left and right multiply the DLMI (13) by $[x^T, w^T, d^T]$ and its transpose to show that V satisfies the following dissipation inequality for all $t \in [0,T]$:

$$\dot{V} + \begin{bmatrix} x \\ \left[\begin{smallmatrix} w \\ d\end{smallmatrix}\right]\end{bmatrix}^T \begin{bmatrix} Q & S \\ S^T & R\end{bmatrix} \begin{bmatrix} x \\ \left[\begin{smallmatrix} w \\ d\end{smallmatrix}\right]\end{bmatrix} + z^T M z \leq -\epsilon\, d^T d. \tag{16}$$

[2] The notation $(\cdot)^T$ in (13) corresponds to an omitted factor required to make the corresponding term symmetric.

Use the choices for (Q,S,R) in (14) to rewrite the second term as $e^Te-\gamma^2d^Td$. Integrate over $[0,T]$ to obtain:

$$x(T)^TP(T)x(T)-x_{G,0}^TP_{11}(0)x_{G,0}+\int_0^T z^T(t)M(t)z(t)dt - (\gamma^2-\epsilon)\|d\|_{2,[0,T]}^2+\|e\|_{2,[0,T]}^2\leq 0.$$

Apply $P(T)\succeq F=0$ and $\Delta\in\mathcal{I}(\Psi,M)$ to conclude:

$$\|e\|_{2,[0,T]}^2\leq x_{G,0}^TP_{11}(0)x_{G,0}+(\gamma^2-\epsilon)\|d\|_{2,[0,T]}^2. \quad (17)$$

Finally, if $x_G(0)=0$ then $\|F_u(G,\Delta)\|_{2,[0,T]}<\gamma$. $\square$

3.4 Robust $\mathcal{L}_2$-to-Euclidean Gain

A similar theorem provides a bound on the $\mathcal{L}_2$-to-Euclidean gain of $F_u(G,\Delta)$. This requires the additional assumptions that $D_{G21}(T)=0$ and $D_{G22}(T)=0$ so that $\mathcal{D}_2(T)=0$. Hence $e(T)=\mathcal{C}_2(T)x(T)$ and the gain from d to $e(T)$ is well-defined. To assess the robust $\mathcal{L}_2$-to-Euclidean gain define (Q,S,R,F) as:

$$\begin{aligned}&Q(t):=0,\ S(t):=0,\ R(t):=-\gamma^2\begin{bmatrix}0_{n_w} & 0\\ 0 & I_{n_d}\end{bmatrix},\\ &F:=\mathcal{C}_2^T(T)\mathcal{C}_2(T)=\begin{bmatrix}C_{G2}(T)^TC_{G2}(T) & 0\\ 0 & 0\end{bmatrix}.\end{aligned} \quad (18)$$

With these choices for (Q,S,R,F) the next theorem is a minor adaptation of Theorem 6 and the proof is omitted.

Theorem 7 *Let G be an LTV system defined by (8) with $D_{G21}(T)=0$ and $D_{G22}(T)=0$. Let $\Delta:\mathcal{L}_2^{n_v}[0,T]\to\mathcal{L}_2^{n_w}[0,T]$ be a given operator. Assume $F_u(G,\Delta)$ is well-posed and $\Delta\in\mathcal{I}(\Psi,M)$. If there exists $\epsilon>0$, $\gamma>0$, and a differentiable function $P:[0,T]\to\mathbb{S}^n$ and such that $P(T)\succeq F$ and*

$$DLMI_{Rob}(P,M,\gamma^2,t)\preceq -\epsilon I\ \ \forall t\in[0,T] \quad (19)$$

then $\|F_u(G,\Delta)\|_{E,[0,T]}<\gamma$.

The condition in Theorem 7 robustly bounds the states $x_G(T)$ reachable by disturbances for any $\Delta\in\mathcal{I}(\Psi,M)$. Note $\mathcal{C}_2(T):=\begin{bmatrix}C_{G2}(T) & 0\end{bmatrix}$ so that $e(T)$ only depends on $x_G(T)$. The IQC filter Ψ is used only for analysis and $x_\psi(T)$ is not considered due to the choice of $\mathcal{C}_2(T)$. Also note that the DLMI condition can be modified to compute robust reachable sets with non-zero initial conditions $x_G(0)\neq 0$, e.g. see Chapter 2 of (Moore, 2015).

3.5 RDE Condition for Robust Performance

Theorems 6 and 7 provide a DLMI (13) to bound the induced $\mathcal{L}_2$ and $\mathcal{L}_2$-to-Euclidean gain of $F_u(G,\Delta)$. More general robust performance conditions can be formulated by proper choice of (Q,S,R,F). The numerical algorithm proposed in Section 4 relies on an equivalence between the DLMI (13) and a related RDE condition. This equivalence is demonstrated with a quadratic cost $\mathcal{J}$ that combines the performance specification (Q,S,R,F) and the IQC (Ψ,M). Specifically, define $\mathcal{J}$ with the extended dynamics in (12): $\dot{x}=\mathcal{A}x+\mathcal{B}\left[\begin{smallmatrix}w\\ d\end{smallmatrix}\right]$. The cost matrices $(\mathcal{Q},\mathcal{S},\mathcal{R},\mathcal{F})$ are chosen as:

$$\mathcal{F}:=F,\quad \begin{bmatrix}\mathcal{Q} & \mathcal{S}\\ \mathcal{S}^T & \mathcal{R}\end{bmatrix}:=(\cdot)^TM\begin{bmatrix}\mathcal{C}_1 & \mathcal{D}_1\end{bmatrix}+\begin{bmatrix}Q & S\\ S^T & R\end{bmatrix} \quad (20)$$

and the quadratic cost associated with these choices is:

$$\begin{aligned}\mathcal{J}\left(\left[\begin{smallmatrix}w\\ d\end{smallmatrix}\right]\right):=&\ x(T)^T\mathcal{F}x(T)+\int_0^T z^T(t)M(t)z(t)dt\\ &+\int_0^T\begin{bmatrix}x(t)\\ \left[\begin{smallmatrix}w(t)\\ d(t)\end{smallmatrix}\right]\end{bmatrix}^T\begin{bmatrix}Q(t) & S(t)\\ S(t)^T & R(t)\end{bmatrix}\begin{bmatrix}x(t)\\ \left[\begin{smallmatrix}w(t)\\ d(t)\end{smallmatrix}\right]\end{bmatrix}dt.\end{aligned}$$

The next corollary states the equivalence between the DLMI and RDE conditions. The DLMI can be rewritten as an RDI by the Schur complement lemma (Boyd et al., 1994). Hence the corollary follows from Theorem 1.

Corollary 8 *Let $(\mathcal{Q},\mathcal{S},\mathcal{R},\mathcal{F})$ be given by (20). The following are equivalent for any $\epsilon>0$ and $\gamma>0$:*

(1) There exists a differentiable function $P:[0,T]\to\mathbb{S}^n$ such that $P(T)\succeq F$ and $DLMI_{Rob}(P,M,\gamma^2,t)\preceq-\epsilon I$.

(2) $\mathcal{R}(t)\prec 0$ for all $t\in[0,T]$. In addition, there exists a differentiable function $Y:[0,T]\to\mathbb{S}^n$ such that $Y(T)=F$ and

$$\dot{Y}+\mathcal{A}^TY+Y\mathcal{A}+\mathcal{Q}-(Y\mathcal{B}+\mathcal{S})\mathcal{R}^{-1}(Y\mathcal{B}+\mathcal{S})^T=0$$

4 Computational Approach

This section describes computational details and presents an algorithm that combines complementary aspects of the DLMI and RDE conditions.

4.1 IQC Parameterization

There is typically an infinite set of valid IQCs for a given uncertainty Δ. Numerical implementations using IQCs often involve a fixed choice for Ψ and optimization subject to convex constraints on M (Megretski and Rantzer, 1997; Veenman et al., 2016; Palframan et al., 2017). Two examples are given below.

Example 9 *Consider an LTI uncertainty $\Delta\in\mathbb{RH}_\infty$ with $\|\Delta\|_\infty\leq 1$. By Example 4, Δ satisfies any IQC*

(Ψ, M) *with* $\Psi := \left[\begin{smallmatrix} \Psi_{11} & 0 \\ 0 & \Psi_{11} \end{smallmatrix}\right]$, $M := \left[\begin{smallmatrix} M_{11} & 0 \\ 0 & -M_{11} \end{smallmatrix}\right]$, *and* $M_{11} \succeq 0$. *A typical choice for* Ψ_{11} *is:*

$$\Psi_{11} := \left[1, \frac{1}{(s+p)}, \dots \frac{1}{(s+p)^v}\right]^T \quad \text{with } p > 0 \tag{21}$$

The analysis is performed by selecting (p, v) *to obtain (fixed)* Ψ *and optimizing over* $M_{11} \succeq 0$. *The results depend on the choice of* (p, v). *Larger values of* v *represent a richer class of IQCs and hence yield less conservative results but with increasing computational cost. Further details are given in Veenman et al. (2016) including a more general parameterization for this class of uncertainties.*

Example 10 *The analysis can incorporate conic combinations of multiple IQCs. Let* (Ψ_1, M_1) *and* (Ψ_2, M_2) *define valid IQCs for* Δ. *Hence* $\int_0^T z_i^T M_i z_i \, dt \geq 0$ *where* z_i *is the output* Ψ_i *driven by* v *and* $w = \Delta(v)$. *For any* $\lambda_1, \lambda_2 \geq 0$ *the two constraints can be combined to yield:*

$$\int_0^T \lambda_1 z_1^T M_1 z_1 + \lambda_2 z_2^T M_2 z_2 \, dt \geq 0 \tag{22}$$

Thus a valid time-domain IQC for Δ *is given by*

$$\Psi := \left[\begin{smallmatrix} \Psi_1 \\ \Psi_2 \end{smallmatrix}\right] \text{ and } M(\lambda) := \left[\begin{smallmatrix} \lambda_1 M_1 & 0 \\ 0 & \lambda_2 M_2 \end{smallmatrix}\right] \tag{23}$$

The analysis optimizes over λ *given selected* (Ψ_i, M_i).

4.2 Analysis with the DLMI Condition

Assume the IQC is (Ψ, M) with Ψ fixed and M constrained to a feasible set $\mathcal{M}$ described by LMIs. The DLMI (13) has the same form for induced $\mathcal{L}_2$ and $\mathcal{L}_2$-to-Euclidean gains but with different choices of (Q, S, R, F). In both cases the DLMI is linear in (P, M, γ^2) for fixed (G, Ψ). The dependence on γ^2 enters via R. The smallest bound on the robust gain can be computed from a convex semidefinite program (SDP):

$$\begin{aligned} &\min \gamma^2 \\ &\text{subject to: } M \in \mathcal{M},\ P(T) \succeq F \\ &DLMI_{Rob}(P, M, \gamma^2, t) \preceq -\epsilon I \ \forall t \in [0, T] \end{aligned}$$

There are two main issues. First, the DLMI corresponds to an infinite number of constraints since it must hold $\forall t \in [0, T]$. This can be approximated by enforcing the DLMI on a grid $t_{DLMI} := \{t_k\}_{k=1}^{N_g} \subset [0, T]$. Second, the optimization requires a search over the space of functions $P : [0, T] \to \mathbb{S}^n$. This is addressed by restricting P to be a linear combination of differentiable bases functions. Let $h_j : [0, T] \to \mathbb{R}$ $(j = 1, \dots, N_s)$ and $H : [0, T] \to \mathbb{S}^n$ be given scalar and matrix differentiable basis functions. The storage function and its derivative are given by:

$$P(t) = \sum_{j=1}^{N_s} h_j(t) X_j + H(t)\, x_{N_s+1} \tag{24}$$

$$\dot{P}(t) = \sum_{j=1}^{N_s} \dot{h}_j(t) X_j + \dot{H}(t)\, x_{N_s+1} \tag{25}$$

Here $\{X_j\}_{j=1}^{N_s} \subset \mathbb{S}^n$ and $x_{N_s+1} \in \mathbb{R}$ are optimization variables. Initial work in (Moore, 2015) used scalar basis functions generated with a cubic spline and no matrix basis function. The spline is constructed with a time grid $\tau_{sp} := \{\tau_j\}_{j=1}^{N_s}$ where $\tau_j < \tau_{j+1}$. Note, the spline grid τ_{sp} and DLMI grid t_{DLMI} can be distinct. The spline consists of $N_s - 1$ cubic functions defined on $[\tau_j, \tau_{j+1}]$. It interpolates the decision variables $\{X_j\}_{j=1}^{N_s}$, i.e. $P(\tau_j) = X_j$. The cubic functions satisfy boundary conditions to ensure continuity of the spline and its first/second derivatives at the interval endpoints. The corresponding bases $\{h_j\}_{j=1}^{N_s}$ are not easy to express in explicit form but they can be evaluated numerically at any $t \in [0, T]$. The algorithm proposed below also uses one matrix basis function H generated by the RDE.

The approximations for the DLMI and P lead to a finite dimensional SDP in variables $\{X_j\}_{j=1}^{N_s}$, x_{N_s+1}, M, and γ^2. The optimization can be performed with standard SDP solvers. Enforcing the DLMI only on a finite grid decreases the optimal cost relative to the original infinite-dimensional SDP. Conversely, restricting P to lie in a finite dimensional subspace increases the optimal cost. The solution accuracy depends on the choice for the constraint time grid and basis functions. A denser time grid and additional bases functions will improve the accuracy but with increased computation time. Unfortunately, the combination of these two approximations, one optimistic and one pessimistic, does not allow us to draw a conclusion in either direction.

4.3 Analysis with the RDE Condition

The RDE conditions for robust induced $\mathcal{L}_2$ and $\mathcal{L}_2$-to-Euclidean gains do not require the constraint and basis function approximations needed for the corresponding DLMI. Specifically for any (G, Ψ, M, γ^2) the RDE can be integrated within a specified numerical accuracy using standard ODE solvers. If the RDE exists on $[0, T]$ when integrated backward from $Y(T) = F$ then the robust gain is less than γ. Bisection on γ can be used to find the smallest bound on the robust gain. The difficulty with the RDE condition is that it has a rational dependence on the IQC matrix M. In most cases it would be inefficient to perform numerical gradient searches over M to find the smallest bound γ. A key benefit of the RDE condition over the DLMI condition is that it provides a guaranteed upper bound on the robust gain.

4.4 Combined Algorithm

Algorithm 1 combines the DLMI and RDE conditions. It is initialized with a stopping tolerance tol, a max number of iterations N_{iter}, a time grid t_{DLMI} to enforce the DLMI, a time grid τ_{sp} for the (scalar) spline basis functions, and a matrix basis function $H \equiv 0$. Reasonable choices for the stopping parameters are $tol = 5 \times 10^{-3}$ and $N_{iter} = 10$. A smaller tolerance and/or additional iterations will typically yield improved answers at the expense of additional computation. The initial time grids can be coarse, e.g. set t_{DLMI} and τ_{sp} as 20 and 10 evenly spaced points in $[0, T]$, respectively. The iteration described further below adaptively adds times to the grid t_{DLMI}. It also uses the RDE solution and matrix basis function H to complement the coarse spline grid τ_{sp}.

The first step is to solve the finite SDP by enforcing the DLMI on t_{DLMI}. This returns, if feasible, $\gamma_{SDP}^{(1)}$, $M^{(1)}$, and the storage function decision variables $\{X_j^{(1)}\}_{j=1}^{N_s}$. The next step is to hold the IQC matrix fixed at $M^{(1)}$ and bisect to find the smallest γ such that the RDE solution exists on $[0, T]$. This yields $\gamma_{RDE}^{(1)}$, $P_{RDE}^{(1)}$, and $t_{RDE}^{(1)}$. Here $t_{RDE}^{(1)}$ denotes the (dense) grid of time points returned by the ODE solver associated with $P_{RDE}^{(1)}$.

Two updates are performed before the next iteration. First, the matrix basis function is set equal to the RDE solution if $\gamma_{RDE}^{(1)} < \infty$. This choice is optimal for $M^{(1)}$ and the use of this matrix basis function significantly reduces the conservatism. At the next iteration the cubic splines are only needed to perturb around $P_{RDE}^{(1)}$. The second update involves the DLMI time grid. If the DLMI time grid is too coarse then $\gamma_{SDP}^{(1)} < \gamma_{RDE}^{(1)}$. In this case the DLMI is evaluated on the (dense) grid of time points $t_{RDE}^{(1)}$. The time points where the DLMI is infeasible (or some subset) are added to t_{DLMI}. The algorithm terminates if the RDE and SDP results are close or the maximum number of iterations has been reached. Otherwise the subsequent iterations proceed in the same fashion. Upon termination, the RDE solution (if feasible at any iteration) provides a guaranteed upper bound on the gain. This also guarantees a solution to the DLMI that holds on all $t \in [0, T]$, and not just on the grid t_{DLMI}.

Algorithm 1 Combined DLMI/RDE Approach

Given: G and Ψ
Initialize: tol, N_{iter}, $t_{DLMI} := \{t_k\}_{k=1}^{N_g}$, $\tau_{sp} := \{\tau_j\}_{j=1}^{N_s}$, and $H \equiv 0$.
for $i = 1 : N_{iter}$ **do**
  Solve SDP: Enforce DLMI on t_{DLMI}. Use spline basis functions defined by τ_{sp} and matrix basis function H.
  Output: $\gamma_{SDP}^{(i)}$, $M^{(i)}$, and decision vars. for P.

  Solve RDE: Hold $M^{(i)}$ fixed and bisect to find smallest γ such that the RDE exists on $[0, T]$.
  Output: $\gamma_{RDE}^{(i)}$, $P_{RDE}^{(i)}$, and $t_{RDE}^{(i)}$.

  Updates:
  If $\gamma_{RDE}^{(i)} < \infty$ then $H := P_{RDE}^{(i)}$ else $H := 0$.
  Add time points to t_{DLMI} if $\gamma_{SDP}^{(i)} < \gamma_{RDE}^{(i)}$.

  If $|\gamma_{SDP}^{(i)} - \gamma_{RDE}^{(i)}| < tol \cdot \gamma_{SDP}^{(i)}$ then terminate.
end for

5 Examples

5.1 Robust Induced $\mathcal{L}_2$ Gain

Consider an uncertain system $F_u(G, \Delta)$ with $\Delta \in \mathbb{RH}_\infty$ and $\|\Delta\|_\infty \le 1$. G is an LTI system defined by:

$$A_G := \begin{bmatrix} -0.8 & -1.3 & -2.1 & -2.5 \\ 2 & -0.9 & -8.4 & 0.7 \\ 2 & 8.6 & -0.5 & 12.5 \\ 2.1 & -0.3 & -12.6 & -0.6 \end{bmatrix} \quad B_G := \begin{bmatrix} -0.6 & 1 \\ 0 & 0.2 \\ 0 & 0.4 \\ -1.3 & -0.2 \end{bmatrix}$$

$$C_G := \begin{bmatrix} -1.4 & 0 & 0.5 & 0 \\ 0 & -0.1 & 1 & 0 \end{bmatrix} \quad D_G := \begin{bmatrix} -0.3 & 0 \\ 0 & 0 \end{bmatrix}$$

The infinite-horizon, worst-case induced $\mathcal{L}_2$ gain is 1.49 as computed with `wcgain` in Matlab. Figure 4 shows finite-horizon robust gains (blue solid) computed using Algorithm 1 for $T := \{1, 2, 5, 10, 20, 30, 40, 50, 100\}$. The red dashed line denotes the infinite-horizon gain of 1.49. Algorithm 1 is initialized for each horizon T with $tol = 5 \times 10^{-3}$, $N_{iter} = 10$, t_{DLMI} as 20 evenly spaced points in $[0, T]$, and τ_{sp} as 10 evenly spaced points in $[0, T]$. The IQC parameterization in Example 9 is used with $v = 1$ and $p = 10$. It took 420 sec to compute all nine finite-horizon results on a standard laptop. The iteration for $T = 5$ sec terminated in 3 steps and all other iterations terminated in 2 steps. Matlab's `LMILab` and `ode45` were used to solve the SDP and integrate the RDE in Algorithm 1. The ODE options were set to have an absolute and relative error of 10^{-8} and 10^{-5}, respectively.

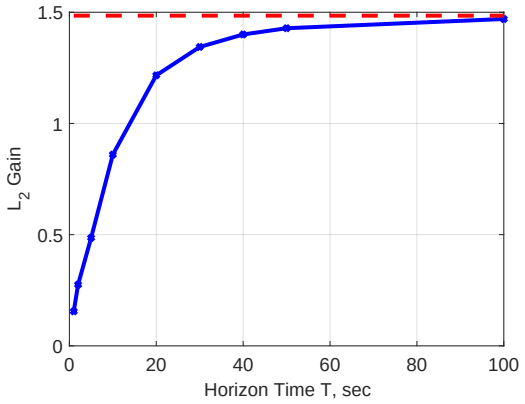

Fig. 4. Robust Induced $\mathcal{L}_2$ Gain vs. Time Horizon (blue) and infinite horizon result (red dashed).

The DLMI is enforced only on the points in t_{DLMI}. This gives 20 LMI constraints on the first iteration but ad-

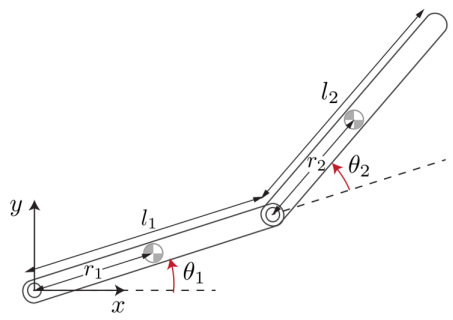

Fig. 5. Two link robot arm (Murray et al., 1994).

ditional constraints as points are added to t_{DLMI}. The number of (scalar) LMI variables is dominated by the variables X_j used to describe $P(t)$ in Equation 24. The extended system (G and Ψ) has $n = 6$ so that each X_j contributes 21 LMI variables. There are $N_s = 10$ basis functions specified by τ_{sp} so this yields a total of 210 LMI variables. The actual number of constraints and variables is slightly higher, e.g. due to the IQC description.

The proposed algorithm computes a gain of 1.22 in 39 sec for the horizon $T = 20$sec. The "approximation" method in Moore (2015) was also used with τ_{sp} given as $N_s = \{10, 20, 30\}$ evenly spaced points and the DLMI enforced on $N_g = 2N_s$ times. This yielded gains $\{1.31, 1.25, 1.24\}$ with computation times $\{6, 69, 401\}$ sec. The approximation improves with increasing N_s and N_g but with significant increases in computation. It is also computationally costly to use the RDE. Simply computing the gain for a given X_{11} using the RDE took 12 bisections for a total computation of 11 sec. These simple results demonstrate the benefits of combining the DLMI and RDE conditions.

5.2 Two-link robot arm

This example considers the robustness of a two link robot arm (Figure 5) as it traverses a finite-time trajectory. The mass and moment of inertia of the i-th link are denoted by m_i and I_i. The robot properties are $m_1 = 3kg$, $m_2 = 2kg$, $l_1 = l_2 = 0.3m$, $r_1 = r_2 = 0.15m$, $I_1 = 0.09kg \cdot m^2$, and $I_2 = 0.06kg \cdot m^2$. The equations of motion (Murray et al., 1994) for the robot are given by:

$$\begin{bmatrix} \alpha + 2\beta\cos(\theta_2) & \delta + \beta\cos(\theta_2) \\ \delta + \beta\cos(\theta_2) & \delta \end{bmatrix} \begin{bmatrix} \ddot{\theta}_1 \\ \ddot{\theta}_2 \end{bmatrix} + \begin{bmatrix} -\beta\sin(\theta_2)\dot{\theta}_2 & -\beta\sin(\theta_2)(\dot{\theta}_1 + \dot{\theta}_2) \\ \beta\sin(\theta_2)\dot{\theta}_1 & 0 \end{bmatrix} \begin{bmatrix} \dot{\theta}_1 \\ \dot{\theta}_2 \end{bmatrix} = \begin{bmatrix} \tau_1 \\ \tau_2 \end{bmatrix} \quad (26)$$

with

$\alpha := I_1 + I_2 + m_1 r_1^2 + m_2(l_1^2 + r_2^2) = 0.4425\, kg \cdot m^2$

$\beta := m_2 l_1 r_2 = 0.09\, kg \cdot m^2$

$\delta := I_2 + m_2 r_2^2 = 0.105\, kg \cdot m^2$.

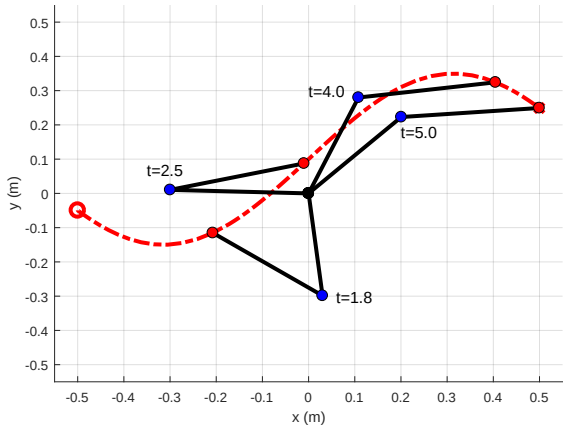

Fig. 6. Desired trajectory in Cartesian coordinates (dotted red line) and robot arm position at four times.

The state and input are $\eta := [\theta_1\ \theta_2\ \dot{\theta}_1\ \dot{\theta}_2]^T$ and $\tau := [\tau_1\ \tau_2]^T$, where τ_i is the torque applied to the base of link i. A trajectory $\bar{\eta}$ was selected for the arm and the required input torque $\bar{\tau}$ was computed. Figure 6 shows the desired trajectory for the tip of arm two (red dashed line) in Cartesian coordinates from $t = 0$ to $T = 5$ sec. The arm positions at four different times are also shown. A plot of trim torque $\bar{\tau}$ can be found in (Moore, 2015).

The robot should track this trajectory in the presence of small torque disturbances d. The input torque vector is $\tau = \bar{\tau} + u + d$ where u is an additional control torque (specified below) to reject the disturbances. The nonlinear dynamics (26) are linearized around the trajectory $(\bar{\eta}, \bar{\tau})$ to obtain an LTV system P:

$$\dot{x}(t) = A(t)x(t) + B(t)\left(u(t) + d(t)\right) \quad (27)$$

where $x(t) := \eta(t) - \bar{\eta}(t)$ is the deviation from the equilibrium trajectory. The state matrices (A, B) were computed via numerical linearization at 400 uniformly spaced points in $[0, 5]$. These matrices are linearly interpolated to obtain the LTV system at any $t \in [0, T]$. (A, B) can be computed at any t via numerical linearization but interpolation reduces the computation time.

Next, a time-varying state feedback law $u(t) = -K(t)x(t)$ is designed to improve the disturbance rejection. The feedback gain is constructed via finite horizon, LQR design with the following cost function:

$$J(x, u) = x(T)^T F x(T) + \int_0^T \begin{bmatrix} x(t) \\ u(t) \end{bmatrix}^T \begin{bmatrix} Q & S \\ S^T & R \end{bmatrix} \begin{bmatrix} x(t) \\ u(t) \end{bmatrix} dt$$

where $Q := \mathrm{diag}(100, 10, 100, 10)$, $R := \mathrm{diag}(0.1, 0.1)$, $S = 0$ and $F := \mathrm{diag}(1, 0.1, 1, 0.1)$. The optimal feedback gain is $K(t) = R^{-1}B(t)^T P(t)$ where $P : [0, T] \to \mathbb{S}^n$ is the solution of the RDE corresponding to (Q, S, R, F) with terminal constraint $P(T) = F$.

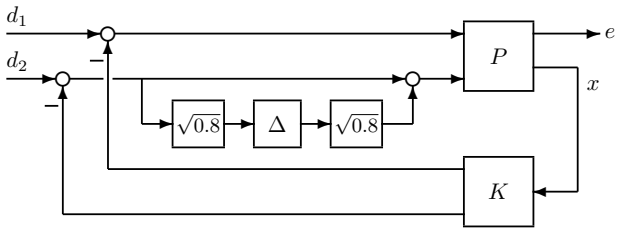

Fig. 7. Uncertain LTV Model for Two-Arm Robot

The analysis aims to bound the final position of the robot arm in the presence of the disturbances d and uncertainty at the joint connecting the two arms. Figure 7 shows a block diagram for the uncertain, linearized robot arm dynamics. $\Delta \in \mathbb{RH}_\infty$ is an LTI uncertainty with $\|\Delta\|_\infty \leq 1$. The factors of $\sqrt{0.8}$ imply that the overall level of uncertainty at the joint is 0.8. Uncertainty is included only at the joint for simplicity and additional uncertainties can be considered if desired. The error signal e contains the two linearized joint angles: $e := [x_1,\, x_2]^T$.

Algorithm 1 was used to compute bounds on the robust $\mathcal{L}_2$-to-Euclidean gain from d to e over the $T = 5$ sec trajectory. The IQC is parameterized as in Example 9 with $v = 1$ and $p = 10$. Algorithm 1 is initialized with $tol = 5 \times 10^{-3}$, $N_{iter} = 10$, t_{DLMI} as 20 evenly spaced points in $[0, T]$, and τ_{sp} as 10 evenly spaced points in $[0, T]$. The algorithm terminated after 3 iterations with a robust gain of $\gamma_{CL} = 0.0588$. It took 55 sec to perform this computation. For comparison, the open-loop robust gain (with $K = 0$) is $\gamma_{OL} = 941.5$. This computation terminated in 7 iterations and took 302 sec. As expected, the feedback significantly reduces the gain.

The results were tested by randomly generating 100 instances of Δ with 0 to 6 states. Each instance of Δ was substituted into Figure 7 to generate a (nominal) LTV closed-loop. The gain was evaluated via bisection with the (nominal) RDE for each sample. The largest gain was 0.0575 achieved with the following uncertainty:

$$\Delta_{wc}(s) = \frac{-0.7861s^2 - 3.383s - 3.631}{0.8s^2 + 3.414s + 3.631}.$$

The linearized closed-loop with Δ_{wc} was simulated with disturbances d such that $\|d\|_{2,[0,T]} \leq \beta := 5$. Figure 8 shows the linearized simulations superimposed on the trim trajectory $\bar{\eta}$. The final outputs $e(T)$ are given by the white dots. The cyan circle corresponds to $\|e(T)\|_2 \leq \gamma_{CL}\beta$. As expected the simulated trajectories terminate in the computed bound (cyan circle). A worst-case disturbance was also constructed for the (nominal) closed-loop with Δ_{wc}. This construction is based on the two-point boundary value problem that connects the performance to the RDE condition (Lemma 11 in Seiler et al. (2017)). A numerically reliable construction is given in (Iannelli et al., 2018). This yields a trajectory that terminates near the boundary of the cyan disk (see zoomed

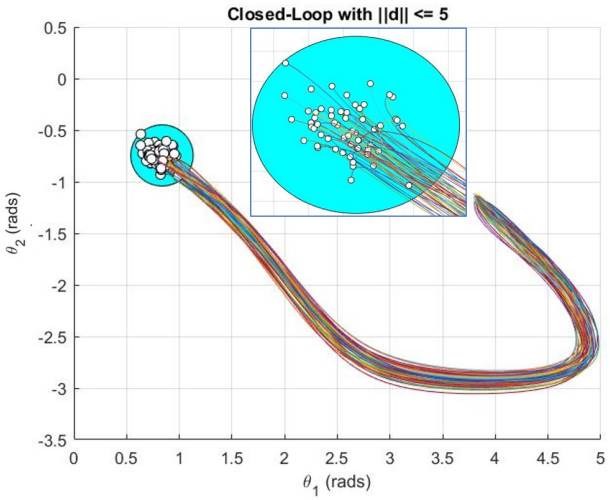

Fig. 8. Closed-loop trajectories in the (θ_1, θ_2) space with Δ_{wc} and random disturbances $\|d\|_{2,[0,T]} \leq 5$. The robust bound on $e(T)$ is also shown (cyan circle).

inset) indicating that the computed robustness bounds are not overly conservative.

6 Conclusions

This paper presented conditions to assess the robustness of uncertain LTV systems over a finite-horizon. The proposed numerical algorithm combines differential linear matrix inequalities and Riccati differential equations. The utility of robust gains was demonstrated with examples including a two-link robot arm.

References

Başar, T. and Bernhard, P. (2008). *H^∞ Optimal Control and Related Minimax Design Problems*. Birkhauser, 3rd edition.

Balakrishnan, V. (2002). Lyapunov functionals in complex μ analysis. *IEEE Transactions on Automatic Control*, 47(9), 1466–1479.

Boyd, S., Ghaoui, L.E., Feron, E., and Balakrishnan, V. (1994). *Linear Matrix Inequalities in System and Control Theory*, volume 15 of *Studies in Applied Math.* SIAM.

Brockett, R. (2015). *Finite Dimensional Linear Systems*. SIAM Classics in Applied Mathematics.

Chen, W. and Tu, F. (2000). The strict bounded real lemma for linear time-varying systems. *Journal of Math. Analysis and Applications*, 244, 120–132.

Fetzer, M., Scherer, C., and Veenman, J. (2017). Invariance with dynamic multipliers. *submitted to the IEEE Trans. on Automatic Control*.

Green, M. and Limebeer, D.J.N. (1995). *Linear Robust Control*. Prentice Hall.

Iannelli, A., Seiler, P., and Marcos, A. (2018). Construction of worst-case disturbances for LTV systems with

application to flexible aircraft. *Submitted to the AIAA Journal of Guidance, Control, and Dynamics*.
Jönsson, U. (2002). Robustness of trajectories with finite time extent. *Automatica*, 38, 1485–1497.
Khalil, H. (2001). *Nonlinear Systems*. Prentice Hall, 3rd edition.
Marcos, A. and Bennani, S. (2009). LPV modeling, analysis and design in space systems: Rationale, objectives and limitations. In *AIAA Guidance, Nav., and Control Conf.*, AIAA 2009–5633.
Masubuchi, I., Kume, A., and Shimemura, E. (1998). Spline-type solution to parameter-dependent LMIs. In *Proceedings of the IEEE CDC*, 1753–1758.
Megretski, A. and Rantzer, A. (1997). System analysis via integral quadratic constraints. *IEEE Transactions on Automatic Control*, 42(6), 819–830.
Moore, R. (2015). *Finite Horizon Robustness Analysis Using Integral Quadratic Constraints*. Master's thesis, University of California, Berkeley.
Murray, R., Li, Z., and Sastry, S. (1994). *A Mathematical Introduction to Robot Manipulation*. CRC Press.
Packard, A. and Doyle, J. (1993). The complex structured singular value. *Automatica*, 29, 71–109.
Palframan, M., Fry, J., and Farhood, M. (2017). Robustness analysis of flight controllers for fixed-wing unmanned aircraft systems using integral quadratic constraints. *IEEE Trans. on Control Systems Tech.*
Petersen, I., Ugrinovskii, V., and Savkin, A. (2000). *Robust Control Design Using H^∞ Methods*. Springer.
Pfifer, H. and Seiler, P. (2015). Robustness analysis with parameter-varying integral quadratic constraints. In *American Control Conference*, 138–143.
Pfifer, H. and Seiler, P. (2016). Less conservative robustness analysis of linear parameter varying systems using integral quadratic constraints. *Int. Journal of Robust and Nonlinear Control*, 26(16), 3580–3594.
Ravi, R., Nagpal, K., and Khargonekar, P. (1991). H_∞ control of linear time-varying systems: A state-space approach. *SIAM J. of Control and Optim.*, 29(6), 1394–1413.
Seiler, P. (2015). Stability analysis with dissipation inequalities and integral quadratic constraints. *IEEE Transactions on Automatic Control*, 60(6), 1704–1709.
Seiler, P., Moore, R., Meissen, C., Arcak, M., and Packard, A. (2017). Finite horizon robustness analysis of LTV systems using integral quadratic constraints. *arXiv:1711.07248*.
Tadmor, G. (1990). Worst-case design in the time domain: The maximum principle and the standard H_∞ problem. *Math. of Control, Signals, and Systems*, 3, 301–324.
van der Schaft, A. (1999). *L_2-gain and passivity in nonlinear control*. Springer-Verlag New York, Inc.
Veenman, J., Scherer, C., and Köroğlu, H. (2016). Robust stability and performance analysis based on integral quadratic constraints. *European Journal of Control*, 31, 1–32.
Willems, J. (1972a). Dissipative dynamical systems part I: General theory. *Arch. for Rational Mech. and Analysis*, 45(5), 321–351.
Willems, J. (1972b). Dissipative dynamical systems part II: Linear systems with quadratic supply rates. *Arch. for Rational Mech. and Analysis*, 45(5), 352–393.
Zhou, K., Doyle, J.C., and Glover, K. (1996). *Robust and Optimal Control*. Prentice-Hall.

Peter Seiler is a professor at the University of Minnesota in the Aerospace Engineering and Mechanics Department. From 2004-2008, he worked at the Honeywell Research Labs on various aerospace and automotive applications. Since joining Minnesota, he has worked on robust control theory with applications to wind turbines, flexible aircraft, and disk drives.

Robert M. Moore is a systems engineer at Raytheon Space and Airborne Systems in El Segundo, CA. He received an M.S. in Mechanical Engineering from UC Berkeley in 2015 under the supervision of Dr. Andrew Packard and a B.S. in Mechanical Engineering from UC Riverside in 2013.

Chris Meissen is a Research Scientist for the Ford Motor Company. He received his Ph.D. in Mechanical Engineering from U.C. Berkeley in 2017 under the supervision of Andrew Packard and Murat Arcak, M.S. from Colorado State University in 2009, and B.S. from Kansas State University in 2007.

Murat Arcak is a professor at U.C. Berkeley in the Electrical Engineering and Computer Sciences Department. He received the 2006 Donald P. Eckman Award from the American Automatic Control Council, the 2007 Control and Systems Theory Prize from the Society for Industrial and Applied Mathematics, and the 2014 Antonio Ruberti Young Researcher Prize from the IEEE Control Systems Society. He is a fellow of IEEE.

Andrew Packard is the Fanuc Chair Professor of Mechanical Engineering at U.C. Berkeley. He is an author of the Robust Control toolbox distributed by Mathworks. The MeyerSound X-10 loudspeaker utilizes novel feedback control circuitry developed by his research group. He received the campus Distinguished Teaching Award, the 1995 Donald P. Eckman Award, the 2005 IEEE Control System Technology Award. He is a fellow of IEEE.